J2.5

MEASUREMENT OF NET OCEAN SURFACE HEAT FLUX, SOLAR IRRADIANCE AND TEMPERATURE DURING THE CBLAST-LOW FIELD PROGRAM USING A NOVEL SURFACE CONTACT MULTI-SENSOR FLOAT

J.P.Boyle*
Western Connecticut State University

1. INTRODUCTION

The author is involved with development of an *in-situ* electromechanical device to measure heat transfer between the atmosphere and ocean (Suomi, *et al.* 1996; Sromovsky, *et al.* 1999a, 1999b; Boyle, 1999, 2000, 2004). The ultimate goal is for multiple, freely floating, autonomous instruments to be deployed from aircraft, research vessels and small boats in support of air-sea flux field experiments and to operate untended providing long-term, continuous measurements of surface heat flux, solar irradiance and water surface temperature.

2. MULTI-SENSOR FLOAT

The critical element is a light, wave-following, surface multi-sensor float (MSF) containing two thin flux plates (Fig. 1). Each flux plate has a thermopile and a thermocouple bonded into a flexible mylar film sandwich. One plate has clear mylar outer layers; the other uses black dyed mylar. The difference in solar absorption properties allows solar irradiance to be distinguished from sensible and evaporative heat fluxes.

Two sheets of fiberglass mesh stretched across the toroid-shaped float support the flux plates. This mesh also acts as a diffuser for solar radiation. Surface tension acting on the mesh balances against buoyancy of the toroid thereby positioning the flux plates in the aqueous conductive sublayer. Two twenty-four gauge bare wires are located 3.175 mm above and below the mesh plane. These are used to detect when flux plates are submerged, i.e., no longer in the conductive sublayer. Measured fluxes from each plate can be decomposed:

$$F_{clear} = F_{LS} - \alpha_c F_{solar,net} + F_{IR,net} \quad (1)$$

$$F_{black} = F_{LS} - \alpha_b F_{solar,net} + F_{IR,net} \quad (2)$$

* *Corresponding author address:* Physics and Meteorology Department, Western Connecticut State Univ. Danbury, CT 06810; e-mail: boylej@wcsu.edu

Figure 1: Multi-sensor floats; Greenland Sea design during testing in NASA wind-wave flume.

where F_{clear}, F_{black} are flux plate values, F_{LS} represents the combined turbulent (latent and sensible) heat flux acting across the thermal sublayer, $F_{solar,net}$ is net solar flux, $F_{IR,net}$ is the net infrared flux, and the α's are empirical solar response coefficients. In this model, nighttime fluxes measured by each flux plate are the same. During the day, the difference in flux plate signals is proportional to net sea surface irradiance.

3. ROOFTOP LABORATORY TESTS

Prior to ocean deployments, several laboratory tests were performed using a rooftop water tank to evaluate MSF solar irradiance and "skin" temperature measurement accuracy. Fig. 2 is a time series of clear and black flux plate signals during a 3 day period. In the upper plot, the daytime black flux plate signal is depressed more than the clear flux plate due to its greater solar absorption. At night clear and black flux plates generally track together. Lower plot shows MSF estimate of net solar flux compared to Eppley Black & White and LI-COR pyranometers.

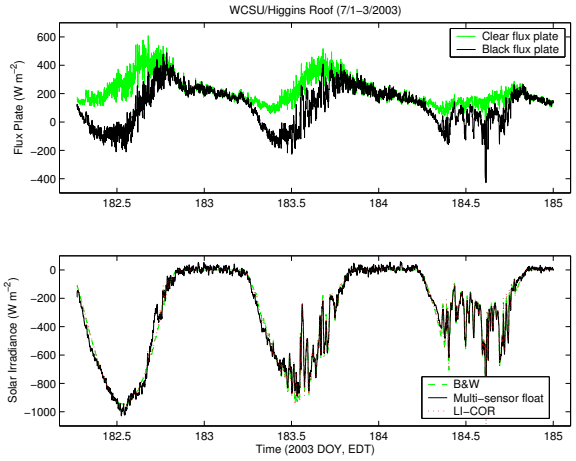

Figure 2: Solar irradiance measurement: comparison of MSF and land-based pyranometer fluxes during clear sky (DOY 182), partly cloudy (DOY 183) and generally overcast (DOY 184) conditions.

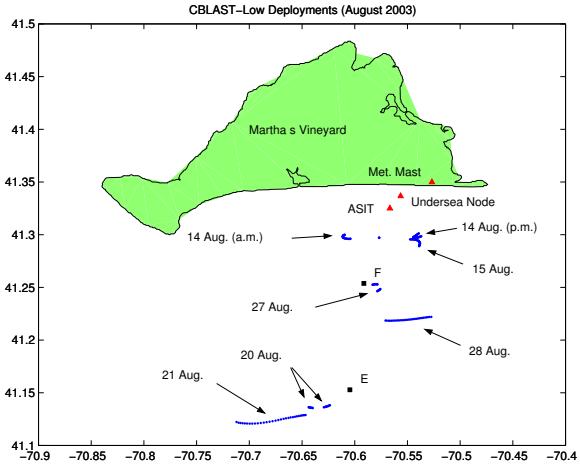

Figure 3: CBLAST-Low Deployments: red triangles are MVCO platforms, black squares are moored IMET buoys and blue circles are guard buoy/MSF drift tracks.

The discrepancy in MSF clear sky solar irradiance measurement on about Day of Year (DOY) 182.3 and 183.3 is due to variable shading of flux plate thermocouple junctions by fiberglass mesh strands. The anomaly from DOY 182.50 to 182.75 (1 July 2003) was observed to be caused by direct beam shadowing of flux plate thermocouple junctions by the upper submergence wire.

4. CBLAST-LOW (AUGUST 2003)

The CBLAST-Low field experiment was performed at the Martha's Vineyard Coastal Observatory (MVCO). MVCO consists of three main elements: an atmospheric component (meteorological mast), an underwater component (undersea node) and the Air-Sea Interaction Tower (ASIT) which spans the air-water interface. Fig. 3 shows the location of MVCO platforms as well as Improved Meteorological (IMET) moored buoys "E" and "F" instrumented for measurement of the components of net surface heat flux. MVCO and IMET measurements provide the reference fluxes and water temperatures to assess the accuracy and performance of MSFs deployed during CBLAST-Low.

Radiometric fluxes are measured using pyranometers and pyrgeometers mounted on the ASIT and moored IMET buoys. Sensible and latent heat flux estimates are calculated using the direct covariance method (ASIT at 2 heights) and two bulk aerodynamic parameterizations (Clayson, *et al.* 1996; Fairall, *et al.* 1996 with modifications from Bradley, *et al.* 2000).

The MSF is deployed tethered, by a 7.62 m floating cable, to a World Ocean Circulation Experiment (WOCE) Lagrangrian drifting buoy. The WOCE buoy is designed to drift with the ocean currents at a depth of 15 m (Sybrandy and Niiler, 1991). Our WOCE type "guard buoy" has been reconfigured for repeated short-term deployments to support development of various MSF designs.

Fig. 4 is a time series for a 3 hour period just after sunrise with clear sky conditions and light winds ($U_{2.2} \approx 3$ m s^{-1}). MSF net surface heat flux is consistent with direct covariance and bulk aerodynamic algorithm results. As seen in the middle plot, the net flux is dominated by the solar radiation component. MSF overestimates clear sky net solar radiation after DOY 226.5 (0800 local). This behavior is due to flux plate thermocouple junction shading by fiberglass mesh strands as seen in Fig. 2.

Fig. 5 shows conditions during the 14 Aug. (evening) deployment. From 1705 to the turning point (1905) the guard buoy/MSF drifts toward the southwest generally against the wind and wind-driven seas – this results in some submergence of MSF flux plates. Two categories of submergence are distinguished: water surging into the mesh area triggering only the submergnce wires and a wave washing over the balance float causing a perturbation in air temperature sensor measurement. After the turning point, the guard buoy/MSF drifts northeast – with wind and seas. Fig. 7 shows time series of guard buoy/MSF drift rate, surface and subsurface currents, fluxes and MSF submergence event

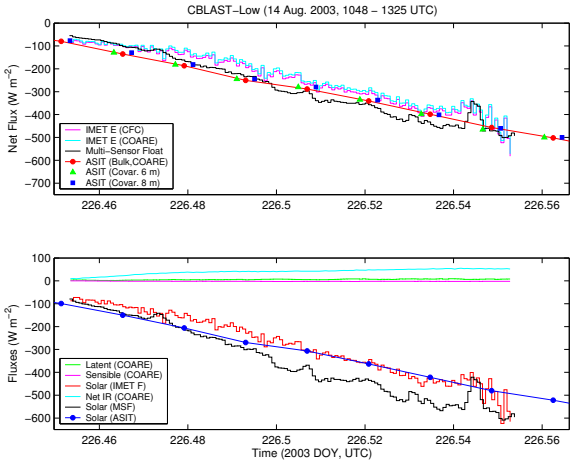

Figure 4: Time series of net surface heat flux (top) and components of net flux (bottom) after sunrise for moored IMET buoy "F", the ASIT and an MSF deployed tethered to a guard buoy (RDB01).

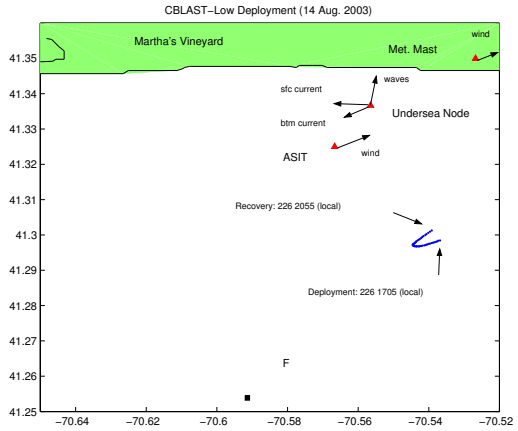

Figure 5: CBLAST deployment: MSF drift track (blue dots) and winds, waves & currents measured by MVCO and moored buoy platforms. The Undersea Node Acoustic Doppler Current Profiler (ADCP) measures bottom currents approximately 3.7 m above the bottom and surface currents approximately 10.7 m from bottom.

fraction. When the guard buoy/MSF trajectory is against wind direction and seas submergence events occur. In this leg, winds are light, $U_{2.2} \approx 2$ m s^{-1}, so submergence events do not appear to invalidate MSF net surface flux measurement. At this time it is unclear why MSF underpredicts the net flux.

Fig. 7 is a time series plot for a 7.5 hour period after sunrise. From the upper plot, it is apparent that the MSF net surface heat flux is consistent with 1 minute values from IMET buoy data and twenty minute means from ASIT bulk and covariance calculations until DOY 233.63. The cause for the MSF flux discrepancy after this time is seen in the middle plot – significant submergence of the MSF flux plates. In this case, submergence events occur for two reasons: the wind speed increases from approximately 5 to 7 m s^{-1} and the wind shifts such that the wind-driven seas are against ocean currents causing choppy seas.

4. SUMMARY

The existing design MSF demonstrates reasonably accurate daytime and nighttime surface heat flux measurement for wind speeds less than approximately 7 m s^{-1} in a variety of environmental conditions. However, this capability depends on avoiding or properly filtering sea-state induced submergence events.

The existing design MSF bulk water temperature measured at a depth of about 1 cm appears to be an accurate meausre of water surface temperature based on comparision with bulk water measurements

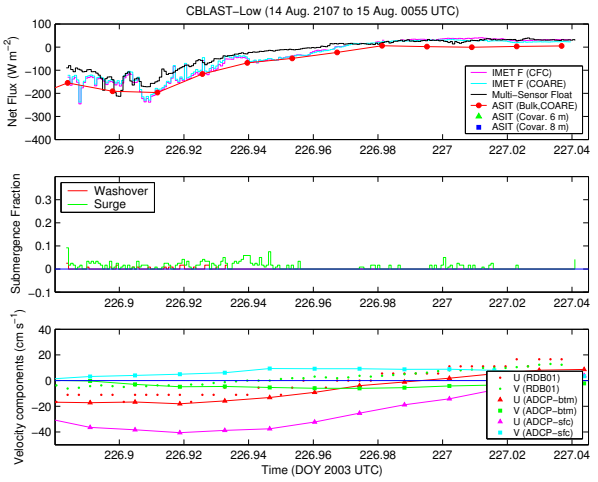

Figure 6: Time series of net surface heat flux (top), flux plate submergence fraction (middle) as well as guard buoy/MSF and MVCO Undersea Node ADCP currents. The guard buoy/MSF is not truely Lagrangian. Mismatches in velocity between the MSF, the wind-driven sea and surface currents cause MSF flux plates to submerge when the wind-driven sea is against guard buoy/MSF drift vector. No direct covariance data are available for this leg.

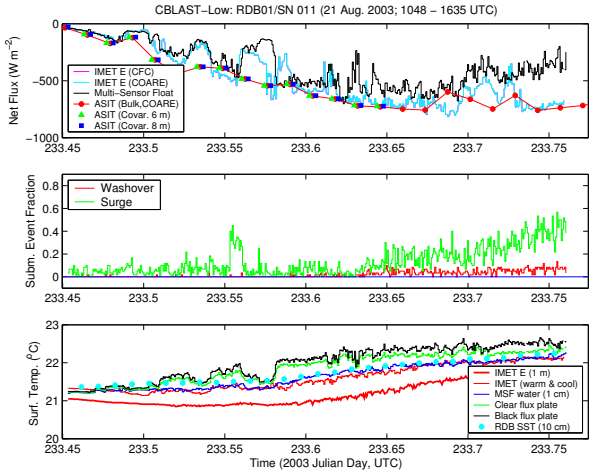

Figure 7: Time series of net surface heat flux (top), flux plate submergence fraction (middle) and ocean surface temperature measurements (bottom) MSF net surface flux compares favorably with ASIT and IMET derived values until the flux plates are submerged more than 20 % of each minute. MSF water temperature measured at ≈ 1 cm depth is consistent with IMET buoy temperature measured at 1 m then corrected for cool skin and warm diurnal layer effects.

made at depths of 1 meter, then corrected for cool skin and warm diurnal layer effects. Clear and black flux plate temperature sensors are exposed to solar radiation and do not appear to be a good measure of water skin temperature.

MSF measurement of sea surface net solar irradiance compares favorably with land-based and buoy-mounted pyranometers in partially cloudy and overcast conditions. In clear sky situations the existing design MSF upper submergence detection wire occasionally casts a shadow on the flux plates. Fiberglass mesh strands shade some of the flux plate thermocouples, degrading the cosine response at low solar elevation angles.

At the present time MSFs cannot be deployed autonomously, but require a guard buoy for power and telecommunications. To minimize wave/current-induced submergence of MSF flux plates, the guard buoy must drift at the same rate as the MSF. The WOCE-type Lagrangrian drifter is not suitable; a new guard buoy must be selected.

References

Boyle, J.P., 2004: Continued Development of an Ocean/Lake Surface Contact Heat Flux, Solar Irradiance and Temperature Sensor *J. Atmos. Oceanic Tech.* Amer. Meteor. Soc., **submitted**.

Boyle, J.P., 2000: Air-Sea Surface Heat Flux, Solar Irradiance and Surface Temperature Measurement using an In-Situ Sensor *10^{th} Conference on Interaction of the Sea and Atmosphere* Amer. Meteor. Soc., p. 31 - 32.

Boyle, J.P., 1999: Solar Radiation Calibration and Modeling Studies for an In-Situ Lake/Ocean Surface Heat Flux Sensor. *10^{th} Conference on Atmospheric Radiation* Amer. Meteor. Soc., pp. 478 - 481.

Bradley, E.F., C.W. Fairall, J.E. Hare, A.A. Grachev, 2000: An Old and Improved Algorithm for Air-Sea Fluxes: COARE 2.6A. *14^{th} Symposium on Boundary Layers and Turbulence* Amer. Meteor. Soc., pp. 294 - 296.

Clayson, C.A., C.W. Fairall, J.A. Curry, 1996: Evaluation of Turbulent Fluxes at the Ocean Surface using Surface Renewal Theory. *J. Geophys. Res.*, 101(C2), pp. 28515 - 28528.

Fairall, C.W., E.F. Bradley, D.P. Rogers, J.B. Edson and G.S. Young, 1996: Bulk Parameterization of Air-Sea Fluxes for Tropical Ocean-Global Atmosphere Coupled Ocean Atmosphere Response Experiment. *J. Geophys. Res.*, 101(C2), pp. 3747 - 3764.

Sromovsky, L.A., Anderson, J.A., Best, F.A., Boyle, J.P., Sisko, C.A., and Suomi, V.E., 1999a: The Skin-Layer Ocean Heat Flux Instrument (SOHFI) I: Design and Laboratory Characterization. *J. Atmos. and Ocean Tech.*, 16(9), 1224 - 1238.

Sromovsky, L.A., Anderson, J.A., Best, F.A., Boyle, J.P. Sisko, C.A., and Suomi, V.E., 1999b: The Skin-Layer Ocean Heat Flux Instrument (SOHFI) II: Field Measurements of Surface Heat Flux and Solar Irradiance. *J. Atmos. and Ocean Tech.*, 16(9), 1239 - 1254.

Suomi, V.E., Sromovsky, L.A., and Anderson, J.A., 1996: Measuring Ocean-Atmosphere Heat Flux with a new In-situ Sensor. *Eighth Conference on Air-Sea Interaction and Symposium on GOALS* Amer. Meteor. Soc., 38 - 42.

Sybrandy, A.L. and P.P. Niiler, 1991: The WOCE/TOGA SVP Lagrangian Drifter Construction Manual, *Scripps Institute of Oceanography*, WOCE Report # 63, 99 pages